Controlling the Electronic Properties of Polythiophene through the Insertion of Nonaromatic Thienyl *S,S*-dioxide Units

G. Barbarella,* L. Favaretto, G. Sotgiu, and M. Zambianchi

Consiglio Nazionale Ricerche, I.Co.C.E.A., Via Gobetti 101, 40129 Bologna, Italy

C. Arbizzani and A. Bongini

Dipartimento di Chimica G. Ciamician, Universitá, Via Selmi 2, 40126 Bologna, Italy

M. Mastragostino

Dipartimento di Chimica Fisica, Universitá, Viale delle Scienze, Parco d' Orleans II, 90128 Palermo, Italy

Received April 27, 1999. Revised Manuscript Received June 14, 1999

A new class of thiophene-based polymers characterized by the presence of one nonaromatic thienyl *S,S*-dioxide moiety (O) to every two, four, and six aromatic thienyl units (T) was prepared from the newly synthesized precursors TOT, TTOTT, and TTTOTTT, and electrochemically characterized. The polymers displayed remarkably greater electron affinities than that of polythiophene and could be reversibly n-doped at moderate potentials, while still maintaining the property of also being p-doped at moderate potential values. All polymers were characterized by good p-doping/undoping cyclability, while at least four aromatic units to every nonaromatic one were needed to ensure good n-doping/undoping cyclability. ZINDO/S//PM3 calculations on TOT, TTOTT, and TTTOTTT and on $(TOT)_3$ and $(TTOTT)_3$, as models for the corresponding polymers, showed that the presence of the nonaromatic units does not affect the π,π^* character of the frontier orbitals but decreases their energy, in particular that of the LUMO. The calculations allow the cyclability properties of the polymers in the p- and n-doping domains to be rationalized in terms of delocalization of the electronic charge of p- and n-type charge carriers over the aromatic units.

Introduction

Polythiophene is one of the most important conjugated organic polymers, characterized by great chemical stability and ease of functionalization which permit the tuning of its many important properties, such as electrical conductivity, electrochromism, fluorescence, electroluminescence, etc.[1] Polythiophene, which is easily oxidized but not easily reduced, is a p-type (hole transporting) semiconductor. Many papers have already been published concerning the way to reduce the band gap of thiophene-based polymers with the hope of making these materials intrinsically conductive.[2] The relationship between the electronic properties and the molecular structure of functionalized polythiophenes has also been explored in hundreds of publications since the late 1980s when the way of making polythiophene soluble by grafting long alkyl chains was found.[1−3] Functionalized polythiophenes are also actively investigated for application in polymeric supercapacitors for energy storage, which require good p- and n-cyclability properties.[4] Owing to the intrinsic difficulty of the n-doping process, there are few conjugated polymers having these characteristics.[5]

Recently, we have reported on the possibility of tailoring the frontier orbitals of thiophene oligomers through the chemical transformation of the thiophene ring into the corresponding thiophene *S,S*-dioxide.[6] Thiophene *S,S*-dioxide[7] is no longer aromatic, has two localized carbon−carbon double bonds and two double

* Author to whom correspondence should be addressed. E-mail: barbarella@area.bo.cnr.it.

(1) *Handbook of organic conductive molecules and polymers*; Nalwa, H. S., Ed.; John Wiley & Sons: Chichester, 1997; Vols. 1−4.

(2) (a) Roncali, J. *Chem. Rev.* **1992**, *92*, 711. (b) Roncali, J. *Chem. Rev.* **1997**, *97*, 173. (c) Mc. Cullogh, R. D. *Adv. Mater.* **1998**, *10*, 93. (d) Huang, H.; Pickup, P. G. *Chem. Mater.* **1998**, *10*, 2212.

(3) (a) Jen, K. Y.; Oboodi, R.; Elsembaumer, R. L. *Polym. Mater. Sci. Eng.* **1985**, *53*, 79. (b) Sato, M.; Tanaka, S.; Kaeriyama, K. *J. Chem. Soc., Chem. Commun.* **1986**, 873. (c) Hotta, S.; Rughooputh, S. D. D. V.; Heeger, A. J.; Wudl, F. *Macromolecules* **1987**, *20*, 212. (d) Patil, A. O.; Ikenoue, Y.; Wudl, F.; Heeger, A. J. *J. Am. Chem. Soc.* **1987**, *109*, 1858. (e) Souto Major, R. M.; Hinkelmann, K.; Eckert, H.; Wudl, F. *Macromolecules* **1990**, *23*, 1268.

(4) (a) Ren, X.; Gottesfeld, S.; Ferraris, J. P. In *Electrochemical Capacitors*; Delnick, F. M., Tomkiewicz, M., Eds.; The Electrochemical Soc., Inc.: Pennington, 1995; Vol. 95-29, p 138. (b) du Pasquier, A.; Gonzales, J.; Sarrazin, C.; Fauvarque, J. F. In *Electrochemical Capacitors II*; Delnick, F. M., Ingersoll, D., Andrieu, X., Naoi, K., Eds.; The Electrochemical Soc., Inc.: Pennington, 1997; Vol. 96-25, p 127. (c) Arbizzani, C.; Mastragostino, M.; Meneghello, L.; Paraventi, R. *Adv. Mater.* **1996**, *8*, 331.

(5) (a) Ferraris, J. P.; Eissa, M. M.; Brotherston, I. D.; Loveday, D. C. *Chem. Mater.* **1998**, *10*, 3528. (b) Arbizzani, C.; Mastragostino, M. In *Current Trends in Polymer Science*; Research Trends: Trivandrum, 1998; Vol. 2, p 217.

10.1021/cm990245e CCC: $18.00
Published on Web 09/03/1999

Scheme 1[a]

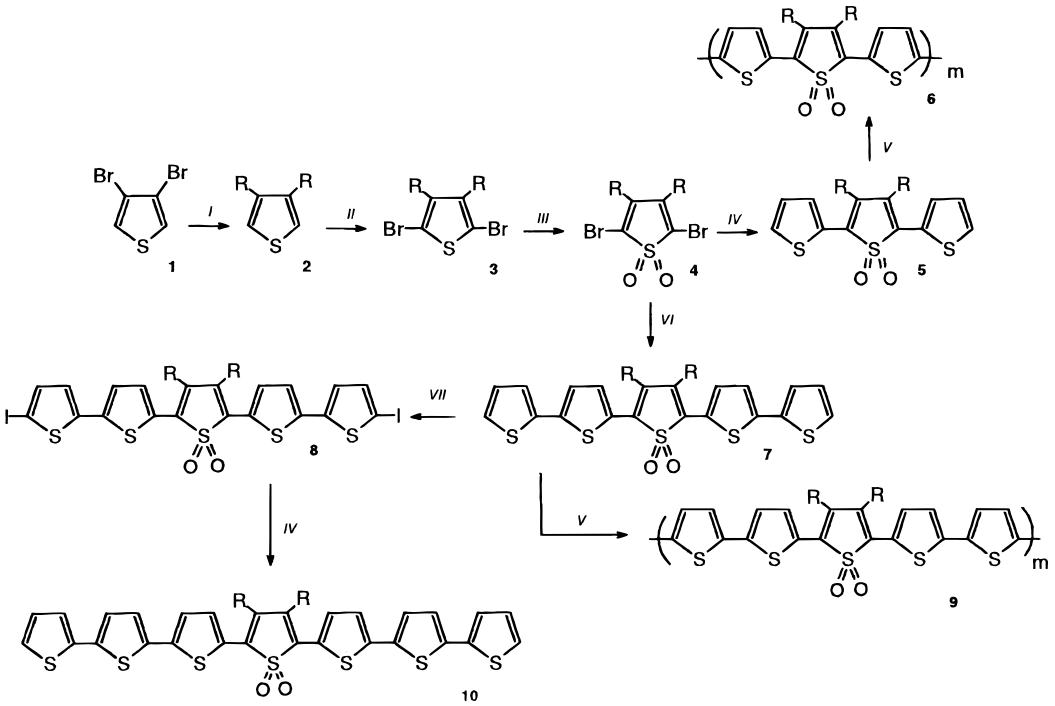

[a] (*i*) $CH_3(CH_2)_5MgBr$, $Ni(dpp)_2Cl_2$, THF. (*ii*) NBS, DMF. (*iii*) MCPBA, CH_2Cl_2. (*iv*) 2-tributylstannylthiophene, $Pd(AsPh_3)_4$, toluene. (*v*) $FeCl_3$, C_6H_6. (*vi*) 5-tributylstannyl-2,2′-bithiophene, $Pd(AsPh_3)_4$, toluene. (*vii*) NIS, DMF.

sulfur−oxygen bonds, and has markedly different optical gap and redox properties from those of the aromatic counterpart, as illustrated below:

$E_{1p,a}$ = 1.89 V*
$E_{1p,c}$ = <- 2.55 V*
λ_{max} = 248 nm

$E_{1p,a}$ = 2.65 V*
$E_{1p,c}$ = -1.44 V*
λ_{max} = 314 nm

* *vs* saturated calomel electrode (SCE)

The insertion of thienyl *S*,*S*-dioxide units into the molecular skeleton of thiophene oligomers leads to an increase in the electron affinity of these compounds, which depends on the number and position of the nonaromatic units.[6a] So far, no attempts have been reported exploiting this possibility to increase the electron affinity of thiophene-based polymers and possibly give them the property of being easily n- and p-dopable.

We are reporting here the synthesis and the electrochemical characterization of a novel class of polythiophenes characterized by the regular alternation of aromatic thienyl rings (T) and nonaromatic thienyl *S*,*S*-dioxide units (O) whose structure is given below (R = hexyl):

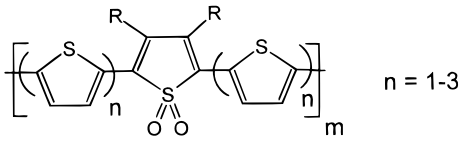

The polymers were prepared chemically and/or electrochemically using as precursors of polymerization the newly synthesized trimer TOT (*m* = 1, *n* = 1, **5**), pentamer TTOTT (*m* = 1, *n* = 2, **7**), and heptamer TTTOTTT (*m* = 1, *n* = 3, **10**) and were characterized by the presence of one nonaromatic thienyl *S*,*S*-dioxide unit every two, four, and six aromatic thienyl rings.

We also report a ZINDO/S//PM3 theoretical study on TOT, TTOTT, and TTTOTTT (R = H, methyl) as models for the precursors of polymerization and on compounds $(TOT)_3$ and $(TTOTT)_3$ (R = H) as models for the polymers, aimed at rationalizing the electronic properties and the p- and n-doping characteristics of the new polymers.

Results

I. Synthesis of TOT, TTOTT, and TTTOTTT (R = Hexyl) and Polymerization of TOT and TTOTT with Ferric Chloride. Scheme 1 gives the synthetic pattern followed for the preparation of the title compounds and the corresponding polymers.

Trimer **5** was obtained in more than 70% yield by the cross coupling of the dibrominated *S*,*S*-dioxide **4** with commercial 2-tributylstannylthiophene in the presence of in situ generated $Pd(AsPh_3)_4$.[6b,c] The UV−vis spectrum of **5** in chloroform (λ_{max} = 415 nm) is given in Figure 1. The maximum wavelength absorption is 60

(6) (a) Barbarella, G.; Favaretto, L.; Zambianchi, M.; Pudova, O.; Arbizzani, C.; Bongini, A.; Mastragostino, M. *Adv. Mater.* **1998**, *10*, 551. (b) Barbarella, G.; Favaretto, L.; Sotgiu, G.; Zambianchi, M.; Antolini, L.; Pudova, O.; Bongini, A. *J. Org. Chem.* **1998**, *63*, 5497. (c) Barbarella, G.; Zambianchi, M.; Sotgiu, G.; Bongini, A. *Tetrahedron* **1997**, *53*, 9401.

(7) (a) Gronowitz, S. *Phosphorus, Sulfur Silicon* **1993**, *74*, 113. (b) Jursic, B. S. *J. Heterocycl. Chem.* **1995**, *32*, 1445. (c) Nakayama, J.; Nagasawa, H.; Sugihara, Y.; Ishii, A. *J. Am. Chem. Soc.* **1997**, *119*, 9077.

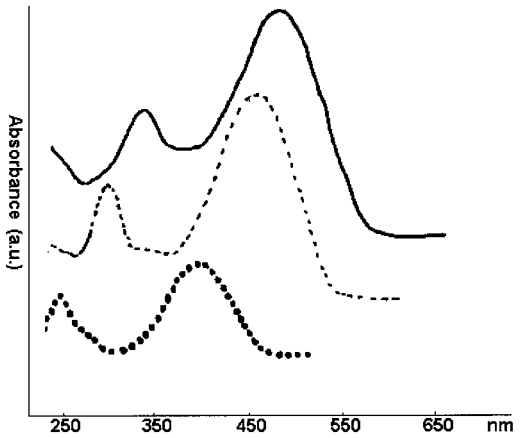

Figure 1. UV−vis spectra in $CHCl_3$ of TOT (**5**, dotted line), TTOTT (**7**, dashed line) and TTTOTTT (**10**, solid line). R = hexyl.

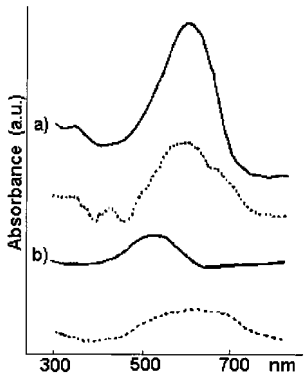

Figure 2. UV−vis spectra of poly(TOT) (**6**) and poly(TTOTT) (**11**, light fraction in CH_2Cl_2 (solid line) and in film cast from CH_2Cl_2 (dashed line). R = hexyl.

nm red shifted with respect to that of terthiophene (λ_{max} = 355 nm).[8] The corresponding polymer, **6**, was obtained by oxidative polymerization with $FeCl_3$ in benzene, according to the modalities employed for the preparation of poly(3-hexylthiophene).[3e,9] Polymer **6** was obtained as a black powder which was moderately soluble in organic solvents. The polydispersity index, measured by gel permeation chromatography with THF as the eluent and polystyrene as the standard, was $M_w/M_n = 1.4$. The shape of the proton NMR spectrum of **6**, characterized, in particular, by the presence of only two sharp doublets in the aromatic region, indicates that the polymer is made prevalently of regioregularly α-linked TOT units. Figure 2a gives the UV−vis spectrum of **6** in CH_2Cl_2 and as a cast film from methylene chloride. The spectrum of the cast film shows the presence of a vibronic fine structure indicating a prevalently planar conformation of the aromatic skeleton, in agreement with what has been observed for regioregular poly(3-hexylthiophene).[10]

(8) (a) Van Pham, C.; Burkhardt, A.; Nkansah, A.; Shabana, R.; Cunnigham, D. D.; Mark, H. B.; Zimmer, H., Jr. *Phosphorus, Sulfur, Silicon Relat. Elem.* **1989**, *46*, 153. (b) Kanemitsu, Y.; Suzuki, K.; Masumoto, Y.; Tomiuchi, Y.; Shiraishi, Y.; Kuroda, M. *Phys. Rev. B.* **1994**, *50*, 2301. (c) Chosrovian, H.; Rentsch, S.; Grebner, D.; Dahm, D. U.; Birckner, E.; Naarman, H.; H. *Synth. Met.* **1993**, *60*, 23.

(9) Sugimoto, R.; Takeda, S.; Gu, H. B.; Yoshino, K. *Chem. Express* **1986**, *1*, 635.

(10) Yamamoto, T.; Komarudin, D.; Arai, M.; Lee, B. L.; Suganuma, H.; Asakawa, N.; Inoue, Y.; Kubota, K.; Sasaki, S.; Fukuda, T.; Matsuda, H. *J. Am. Chem. Soc.* **1998**, *120*, 2047.

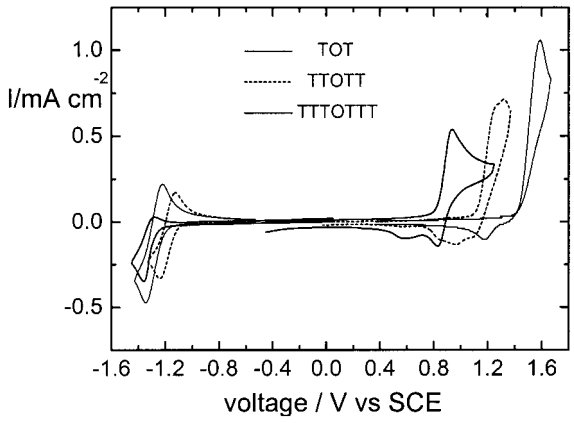

Figure 3. CVs of 1×10^{-3} M TOT (**5**), TTOTT (**7**), and TTTOTTT (**10**) on Pt electrode in CH_2Cl_2−0.2 M $TEABF_4$ at 100 mV s^{-1}. R = hexyl.

Pentamer **7** was obtained by the cross coupling of the dibrominated *S*,*S*-dioxide **4** with the monostannane of 2,2′-bithiophene in 76% yield. The UV spectrum in chloroform is given in Figure 1. As in the case of trimer **5**, the maximum wavelength absorption of **7** (λ_{max} = 469 nm) is markedly red shifted with respect to that of quinquethiophene (λ_{max} = 414 nm).[8]

Pentamer **7** was polymerized using ferric chloride in benzene. The corresponding polymer **9** was obtained in the form of a black powder, insoluble in organic solvents, from which we were only able to extract a very small amount of a light fraction identified as being prevalently made (>90%) of the α-linked decamer. The UV−vis spectrum of this fraction in methylene chloride and that of the corresponding cast film are given in Figure 2b. The cast film of the decamer shows a less resolved vibronic structure than that of polymer **6**, indicating a less rigid and planar polymer skeleton, in agreement with the presence of a smaller number of "rigidifying" thienyl *S*,*S*-dioxide units.[6b]

Heptamer **10** was obtained by the cross coupling of the diiodo derivative **8** with 2-tributylstannylthiophene and $Pd(AsPh_3)_4$ as the catalyst. The reaction yield (30%) was poor, since the metal−halogen exchange reaction became competitive with the cross coupling resulting in the formation of short polymeric chains. The attempt to synthesize **10** by reacting the dibromo derivative of **5** with the monostannane of 2,2′-bithiophene resulted in an even lower yield in heptamer. Heptamer **10** was obtained as a brown powder soluble in most organic solvents. The UV−vis spectrum in chloroform is given in Figure 1. The maximum wavelength absorption (λ_{max} = 505 nm) is markedly red shifted with respect to that of a dialkylated heptathiophene[11] for which we measured λ_{max} = 435 nm. Owing to the low reaction yield, no attempts were made to polymerize **10** with ferric chloride.

II. Electrochemical Characterization and Electropolymerization of 5, 7, and 10. The cyclic voltammetries (CVs) of **5**, **7**, and **10**, on Pt electrode in CH_2Cl_2−0.2 M $TEABF_4$, are given in Figure 3 and the oxidation and reduction potentials vs saturated calomel electrode (SCE) are given in Table 1.

(11) Ten Hoeve, W.; Wynberg, H.; Havinga, E. E.; Meijer, E. W. *J. Am. Chem. Soc.* **1991**, *113*, 5887.

Table 1. Oxidation ($E_{p,a}$) and Reduction ($E_{p,c}$) Potentials,[a] Experimental,[b] and ZINDO/S//PM3 Calculated[c] λ_{max} Values and HOMO and LUMO Energies (E_{HOMO}, E_{LUMO})[d] of 5, 7, 10 and of the Corresponding Polymers

item	$E_{p,a}$	$E_{p,c}$	E_{HOMO}	E_{LUMO}	λ_{max} calc	λ_{max} exp
TOT (**5**)	1.59	−1.35	−7.34	−1.28	409	415
TTOTT (**7**)	1.33	−1.24	−6.86	−1.38	473	469
TTTOTTT (**10**)	0.94	−1.36	−6.67	−1.41	495	505
poly(TOT) (**6**)	1.10	−1.20				575
poly(TTOTT) (**9**)	1.08	−1.34				585
poly(TTTOTTT) (**11**)	0.98	−1.35				575

[a] In volts vs SCE from the oxidation peak and the reduction peak of the CVs. For **5**, **7**, and **10** CVs on Pt in CH_2Cl_2−tetraethylammonium fluoborate ($TEABF_4$) 0.2 M, 1×10^{-3} M oligomer concentration, $v = 100$ mV s^{-1}. For **6** (yielded by casting) and **9** and **11** (by electrosynthesis) on Pt: CVs in propylene carbonate (PC), $TEABF_4$ 0.2 M, $v = 50$ mV s^{-1}. [b] In nanometers. For **5**, **7**, and **10** in $CHCl_3$. Polymer films, yielded by casting (**6**) and electrodeposition (**9** and **11**), on transparent tin oxide electrodes, in PC-$TEABF_4$−0.2 M (**6** and **9**) and air (**11**). [c] For **5**, **7**, and **10** (R = CH_3). [d] In electronvolts. For **5**, **7**, and **10** (R = CH_3).

On increasing the oligomer length the oxidation potential decreases progressively from 1.59 V to 1.33 V and 0.94 V, according to the same trend observed for "fully aromatic" oligothiophenes on increasing the π-conjugation.[12] However, the oxidation potentials for **5**, **7**, and **10** are higher than those reported for oligothiophenes of comparable length. Indeed, the oxidation potential measured for **5** is more than 0.5 V higher than that of α-linked terthiophene (0.95 V, in CH_2Cl_2−tetrabutylammonium hexafluophosphate ($TBAPF_6$) vs Ag/AgCl).[12] The oxidation potentials for unsubstituted quinque- and heptathiophene are not available, but those reported for quater- and sexithiophene (0.80 and 0.65 V, in CH_2Cl_2−$TBAPF_6$ vs Ag/AgCl)[12] are both smaller than that of **10**. By contrast, the range of variation of the reduction potentials of **5**, **7**, and **10** (−1.35, − 1.24, and −1.36 V, respectively) is narrow and suggests the presence of different effects operating in opposite directions. More importantly, these reduction potential values are remarkably less negative than those of unsubstituted oligothiophenes of similar length (−2.07 and −1.91 V vs Ag/AgCl for ter- and quaterthiophene, respectively).[12]

From oligomers **5**, **7**, and **10**, the corresponding polymers **6**, **9**, and **11** were electrochemically synthesized by CVs in CH_3CN and CH_2Cl_2. The electrogrowth of the polymer films was demonstrated by the continuous increase, starting from the second cycle, of a reversible oxidation peak at potentials less positive than that of the corresponding starting molecule. The electrochemical polymerization yielded the best polymer starting from **7** in CH_3CN−tetraethylammonium tetrafluoroborate ($TEABF_4$)−1×10^{-3} M pentamer. All polymers undergo reversible p- and n-doping. Table 1 gives the oxidation and first reduction potentials from CVs in propylene carbonate (PC)−0.2 M $TEABF_4$ of the electrogenerated **9** and **11** polymer films and the chemically synthesized and cast polymer **6** film on Pt, while the corresponding CVs in the anodic and cathodic domains are reported in Figure 4. The electrosynthesis

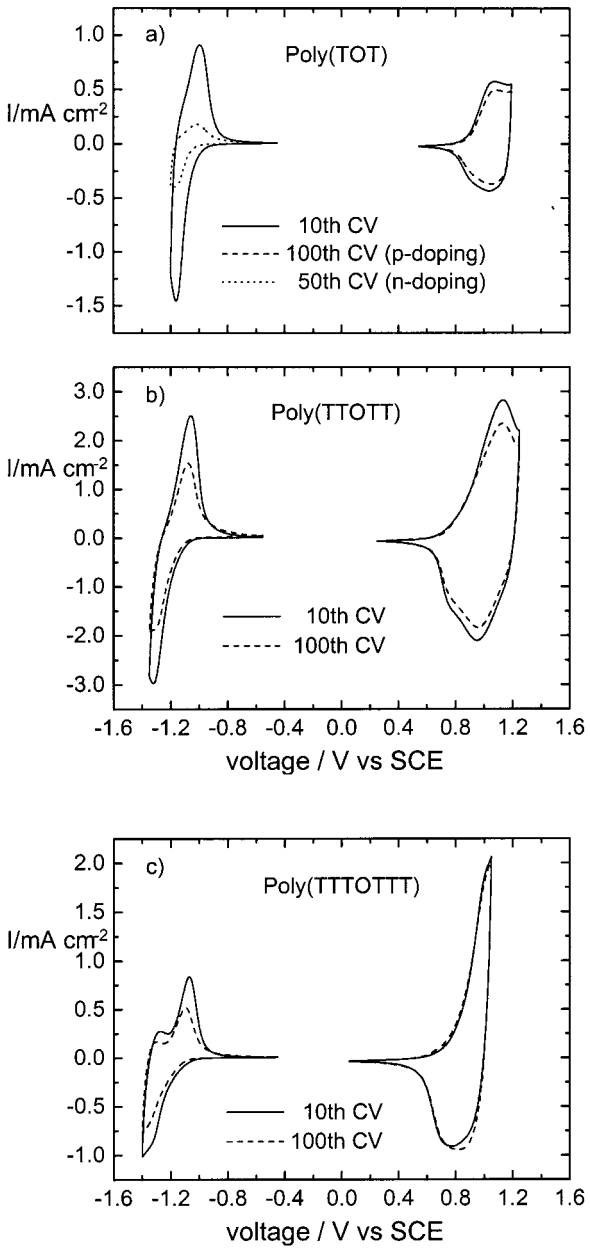

Figure 4. CVs at 50 mV s^{-1} in PC−0.2 M $TEABF_4$ of (a) poly(TOT) (**6**, by casting on Pt), (b) poly(TTOTT), (**9**, electrosynthesized by CV on Pt), and (c) poly(TTTOTTT) (**11**, galvanostatically electrosynthesized on Pt). R = hexyl. The Coulombic efficiencies of the p- and n-doping process from the 10th CV of polymers **6**, **9**, and **11** are 98%, 96%; 98%, 100%; and 96%, 99%, respectively.

charge of **9** was 70 mC cm^{-2} which gave a coverage of 2.8×10^{-7} mol cm^{-2}. In the p- and n-doping domains the 10th cycle undoping charges were −18.9 mC cm^{-2} (doping level, yield % = 70) and +10.0 mC cm^{-2} (yield %= 37), respectively. In the case of **11**, the calculation of the coverage was quite difficult because part of the polymer detached from the Pt electrode in passing from the electrosynthesis to the cycling solution. The p- and n-undoping charges were −7.3 and +3.8 mC cm^{-2}. The p- and n-undoping charges of the cast film **6** were −2.7 and +2.6 mC cm^{-2}, respectively. Note that the polymer oxidation potential changes by moving from the electrosynthesis solution to the PC solution, so that a comparison must be done only among **5**, **7**, **10** and **6**, **9**,

(12) Meerholiz, K.; Heinze, J. *Electrochim. Acta* **1996**, *41*, 1839.

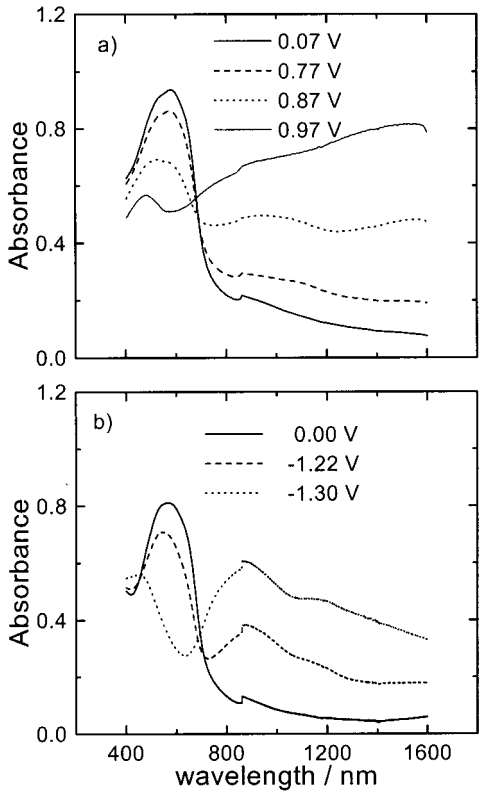

Figure 5. UV−vis spectra of polymer **9** electrosynthesized by CV with 20 mC cm^{-2} in PC−0.2 M $TEABF_4$ at different potentials.

11, separately. (A comparison between **10** and **11** could, indeed, bring to the erroneous conclusion that no polymer is formed.) A confirmation of the polymer formation was also given by the experimental λ_{max} values in Table 1. Whereas the λ_{max} of the starting molecules increases from 415 to 505 nm with the increase of the ring number, the λ_{max} of the polymers are all in the range of 575−585 nm.

The oxidation potentials of **6**, **9**, and **11** are in a more narrow range than that of the corresponding oligomers. The oxidation values are comparable to those of polythiophene and its alkylated derivatives. For example poly(3,4-disubstituted)thiophenes with R3 = R4 = CH_3 or C_2H_5 have oxidation peak potentials of 1.00 and 1.10 V vs SCE. [2a] Also the range of variation of the reduction potentials is narrow, but all the values are remarkably less negative than the reduction potential of polyalkylated oligothiophenes and even of several polythiophenes functionalized with electron withdrawing groups, such as poly(3-*p*-X-phenylthiophene) derivatives with X = CF_3 or SO_2CH_3.[2,5b]

The occurrence of the reversible p- and n-doping processes was demonstrated by the UV−vis spectra of **6** and **9** recorded at different potentials in the anodic and cathodic domains and by the cyclic voltabsorptometries (CVAs). As an example, Figures 5 and 6 give the UV−vis spectra and the CVAs of **9**. The figure shows that as the oxidation potential becomes more positive (Figure 5a) and the reduction potential becomes more negative (Figure 5b) the π,π^* absorption band at 585 nm progressively decreases in intensity and new bands parallelly increase in the near-IR region, following the increase of p- and n-doping levels of the polymer, respectively. The evolution of the polymer electronic

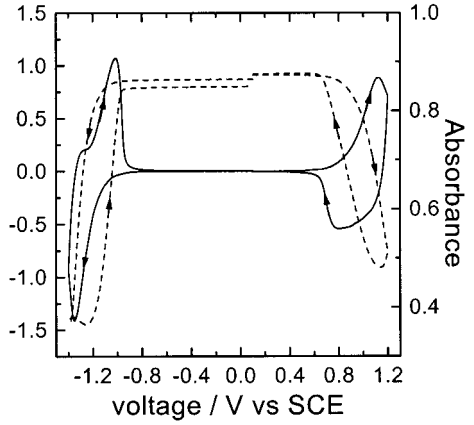

Figure 6. CVs (solid line) at 50 mV s^{-1} in PC−0.2 M $TEABF_4$ of polymer **9** electrosynthesized by CV with 19 mC cm^{-2}. Optical responses (dotted line) recorded at the wavelength of the maximum of the π,π^* transition during the CVs.

structure is reversible, as demonstrated by the CVAs of Figure 6, recorded at the wavelength of the maximum $\pi-\pi^*$ absorption.

Repeated cycles on **6**, **9**, and **11**, carried out in the p- and n-doping domains (Figure 4), showed that the p- and n-doping/undoping processes can occur over many cycles. The figure shows that all polymers satisfactorily perform to repeated cycles in the p-doping domain. However, the same is not true for repeated cycles in the n-doping domain. Indeed, the n-doping/undoping cyclability of **6** is worse than that of **9** and **11**. Polymer **6**, which has one nonaromatic unit every two aromatic ones, after 50 cycles is able to cycle only 30% of the initial (10th CV) charge. Increasing the number of aromatic units leads to much better n-doping/undoping cyclability. Indeed, polymers **9** and **11** are able to cycle after 100 CVs 70% of the initial cycled charge.

III. ZINDO/S//PM3 Semiempirical Calculations. The calculations of the UV spectra and of the shape of the HOMO and LUMO orbitals were carried out using the ZINDO/S Hamiltonian[13] on optimized PM3 geometries. In our experience, among all the semiempirical Hamiltonians, it is the PM3[14] that better reproduces the experimental geometries of thiophene derivatives.

The ZINDO/S//PM3 calculated λ_{max} values and the HOMO and LUMO energies of TOT, TTOTT, and TTTOTTT with R = methyl are given in Table 1, together with the experimental data for the corresponding compounds with R = hexyl.

The configurational interaction analysis (CI) showed that the lowest energy band of the UV−vis spectrum of TOT, TTOTT, and TTTOTTT is due to an almost pure π,π^* HOMO−LUMO transition, which is progressively red shifted on increasing the oligomer length. Interestingly, in the 250−300-nm region, well-defined bands can be observed which are not present in the UV−vis spectra of the corresponding oligothiophenes[8] and which are particularly intense in the case of the trimer. The CI analysis showed that the intense high energy band near 250 nm in the spectrum of TOT (Figure 1) is essentially due to the n,σ^*_{S-O} transition involving the sulfonyl group. The high energy band present in the

(13) Anderson, W. P.; Edwards, W. D.; Zerner, M. C. *Inorg. Chem.* **1986**, *25*, 2728.
(14) Stewart, J. J. P. *J. Comput. Chem.* **1989**, *10*, 209.

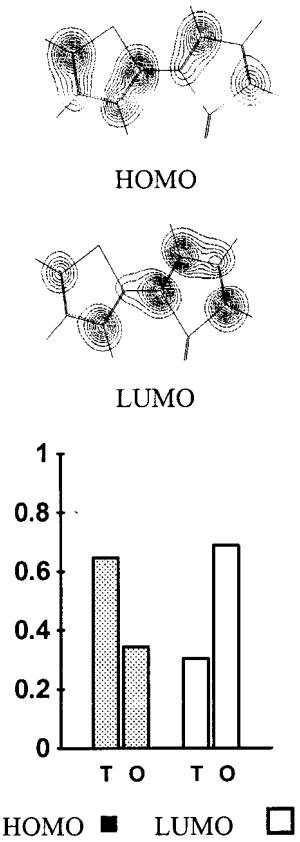

Figure 7. ZINDO/S//PM3 calculated electronic density distribution (top) and the corresponding bar representation (bottom) of the HOMO and LUMO orbitals of TO. In the bar representation, each bar gives the sum of the square of the orbital coefficients for every atom of the aromatic (T) and nonaromatic (O) ring.

spectrum of TTOTT and TTTOTTT near 300 and 340 nm, respectively, is composed of the same (but less intensive) transition and π,π^* transitions involving next HOMO and/or next LUMO orbitals.

To have deeper insight on the effect of the thienyl sulfur functionalization on the electronic distribution, we calculated the electronic density distribution of the HOMO and LUMO orbitals of TO, TOT, TTOTT, TTTOTTT, $(TOT)_3$, and $(TTOTT)_3$ with R = H. In the case of TO, we report in Figure 7 the density distribution for every atom (top) together with a synthetic bar representation (bottom). In the bar representation, each bar gives the sum of the square of the coefficients for every atom of the aromatic and nonaromatic rings. The bar representation allows easily visualization of the point that about 65% of the electronic charge of the HOMO of TO is concentrated on the aromatic ring while nearly 70% that of the LUMO is concentrated on the nonaromatic ring. Figure 8 gives the bar representation of the electronic density distribution of the HOMO and LUMO orbitals of TOT, TTOTT, and TTTOTTT. For comparison, the bar representation of TTT is also reported. Figure 8 shows that the electronic charge of the HOMO displays a tendency to concentrate in the thienyl rings and that of the LUMO in the thienyl *S,S*-dioxide units. The comparison with the trend observed for terthiophene TTT allows one to appreciate the extent of the electronic reorganization following the chemical transformation of the inner ring of the "fully aromatic" thiophene oligomers into the corresponding *S,S*-dioxide.

To have an idea of what happens when more than one TOT or TTOTT molecule is linked together to form a regular polymer, the electronic charge distribution of the model systems TOT−TOT−TOT and TTOTT−TTOTT−TTOTT have also been calculated. It can be safely assumed that the electronic distribution observed for the inner unit of these compounds represents a reasonable approximation of what happens in the polymers obtained from TOT or TTOTT as the precursors. Figure 9 gives the bar representation of $(TOT)_3$ and $(TTOTT)_3$, together with the bar representation of the SOMO of the radical cation and radical anion obtained from the same compounds. The figure shows that the electronic charge of the HOMO of the internal group of both $(TOT)_3$ and $(TTOTT)_3$ is prevalently concentrated in the thienyl units (74 and 87% of the total charge of the internal group, respectively). The electronic charge of the LUMO is distributed at 50% over the thienyl *S,S*-dioxide moiety and at 50% over the two thienyl units in $(TOT)_3$ and at 39% over the thienyl *S,S*-dioxide moiety and at 61% over the four thienyl units in $(TTOTT)_3$. As far as the SOMO of the radical anion and radical cation of $(TOT)_3$ and $(TTOTT)_3$ are concerned, the electronic distribution remains qualitatively that of the HOMO and LUMO orbitals of the corresponding neutral molecules, despite the fact that the structure of the radicals assumes a prevalently quinoidic character.

Finally, the calculations showed that in TOT, TTOTT, and TTTOTTT, the HOMO electronic density of the α-carbons of the terminal rings was remarkably greater than that of the adjacent *β*-carbon. The same was also found in the SOMO of the radical cation derived from the three compounds. This result is in agreement with proton NMR data of polymers **6** and **9**, indicating that the polymerization occurs prevalently through the formation of α−α′-links.

Discussion

As expected,[6a] precursors **5**, **7**, and **10** are characterized by greater electron affinities and ionization energies than those of the corresponding "fully aromatic" counterparts, as deduced from their reduction and oxidation potentials reported in Table 1. However, while the oxidation potential increases progressively with increasing the oligomer length, the reduction potentials of **5**, **7**, and **10** are very similar and apparently almost independent of the oligomer length (see Figure 3). The phenomenon can be rationalized on the basis of the theoretical calculations, since the reduction potential is related to the characteristics of the LUMO and the oxidation potential is related to those of the HOMO. Thus, while in "fully aromatic" oligothiophenes the electronic charge of the LUMO is almost equally distributed over the thienyl rings, in TOT, TTOTT, and TTTOTTT it is mostly concentrated over the thienyl *S,S*-dioxide moiety. Figure 8 shows that even in the last compound, with six thienyl rings, 44% of the electronic charge of the LUMO is still concentrated over the nonaromatic internal ring. However, this effect is counteracted by the tendency of the electronic charge of the LUMO to be delocalized over the thienyl rings. The result of this balance of factors is that the reduction potential of heptamer **10** is very close to that of trimer **5** and more negative than that of pentamer **7**.

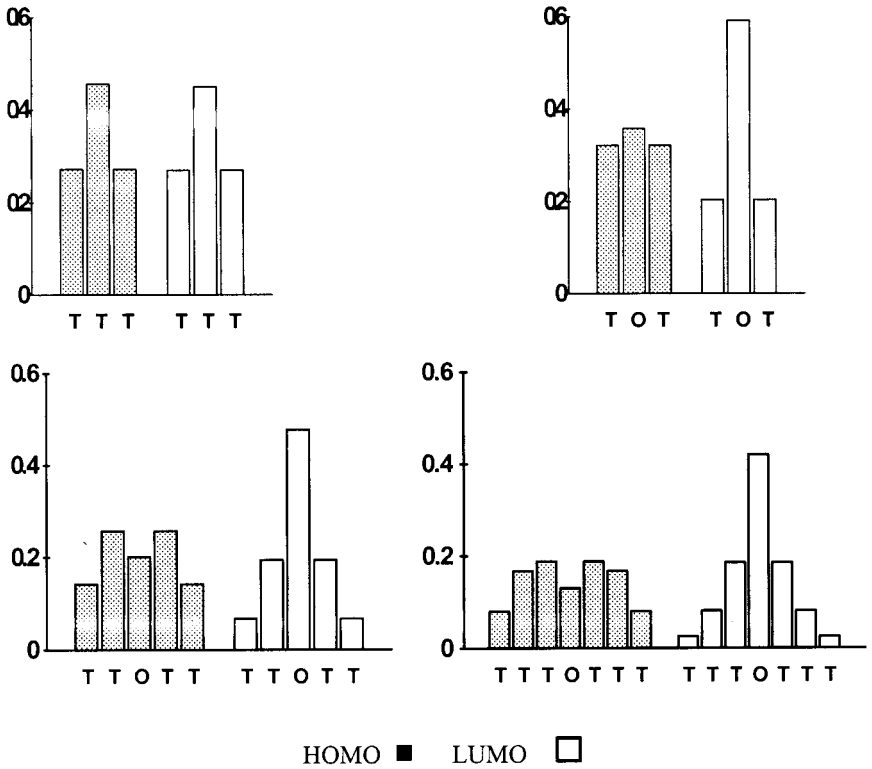

Figure 8. Bar representation of the ZINDO/S//PM3 calculated electronic density distribution of the HOMO and LUMO orbitals of terthiophene TTT and of TOT, TTOTT, and TTTOTTT.

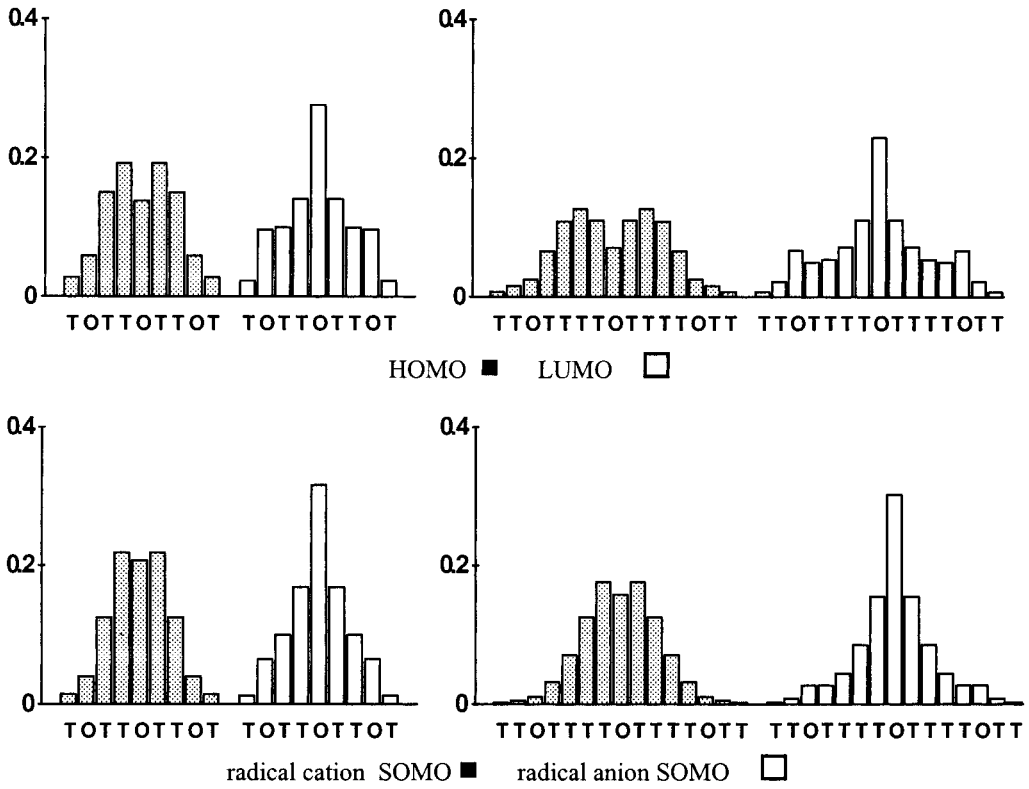

Figure 9. Bar representation of the ZINDO/S//PM3 calculated electronic density distribution of the HOMO and LUMO orbitals of $(TOT)_3$ and $(TTOTT)_3$, together with the bar representation of the SOMO of the corresponding radical cation and radical anion.

The oxidation potentials of **5**, **7**, and **10**, which are similar to those of thiophene (1.7 V[12]), bithiophene (1.25 V[12]), and terthiophene (0.95 V[12]), respectively, range from 1.59 to 0.94 V. The polymerization cancels the differences in the oxidation potentials observed for the precursors. Polymers **6**, **9**, and **11**—which can be viewed as polythiophenes in which one every two, four, and six thienyl rings has been selectively dearomatized through the formation of the corresponding *S*,*S*-dioxide—have very similar oxidation potentials, which are comparable to those of most alkylated polythiophenes. By contrast, the reduction potentials of **6**, **9**, and **11** are remarkably

less negative than those of polythiophene and its alkylated derivatives, indicating a much greater electron affinity of these polymers.

Significantly, the reduction potentials of **6**, **9**, and **11** are similar to those of the corresponding precursors and are even not very different from the reduction potential of 2,5-bis(dimethyl-*tert*-butylsilyl)thiophene *S*,*S*-dioxide.[6a] Again, the calculations offer a key to the interpretation of the phenomenon. Figure 9 shows indeed that, on passing from TOT to TOT−TOT−TOT, the amount of LUMO's electronic charge on the thienyl *S*,*S*-dioxide ring of the internal triad changes from 59% to 50%, whereas on passing from TTOTT to TTOTT−TTOTT−TTOTT, it changes from 48% to 39%, respectively. Thus, despite the delocalization over the lateral triads, the electronic charge of the LUMO is still concentrated to a large extent over the internal thienyl *S*,*S*-dioxide unit.

As shown in Figure 4, polymers **6**, **9**, and **11** undergo reversible p-doping and satisfactorily perform to repeated cycles in the anodic domain, a characteristic which is typical of most polythiophenes. However, and more importantly, all polymers also undergo reversible n-doping. Figure 4 shows that the cyclability performance of the n-doping process is greatly dependent on the relative number of aromatic and nonaromatic units present in the polymer. Polymer **11**, with one nonaromatic unit to every six aromatic ones performs best and polymer **6** with one nonaromatic unit to every two aromatic ones performs worst in the n-doping domain. Polymer **9**, characterized by the presence of one nonaromatic unit to every four aromatic ones, has very similar characteristics to those of polymer **11** and represents, as a consequence, the best compromise between ease of synthesis of the precursor and n-doping/undoping cyclability of the corresponding polymer.

The better cyclability in the n-doping domain of the polymers with the greater number of aromatic units is easily explained by looking at Figure 9. Indeed, the calculations show that the electronic charge distribution of the SOMO of the radical anion derived from the model compounds $(TOT)_3$ and $(TTOTT)_3$ is concentrated to a large extent over the polar thienyl *S*,*S*-dioxide units and in a greater amount in $(TOT)_3$ than in $(TTOTT)_3$. Thus, it can be inferred that the larger amount of negative charge on the nonaromatic units of polymer **6** is likely to cause more extensive charge trapping phenomena (and then overreduction effects in the subsequent cycles, which negatively affect the cyclability performance) than in the other two polymers, in which the charge is more delocalized over the aromatic units.

The property of undergoing reversible n-doping at moderate potential values, while retaining also the property of easy p-doping, and the efficiency characteristics of the n-doping/undoping processes make **9** and **11** interesting materials in the field of symmetric electrochemical devices. The loss of cyclable charge (see Figure 4) is comparable to that reported so far for many n-doped conjugated polymers.[5] Work is in progress on this point. Low cost synthesis and the possibility of a great number of easy structure modifications to increase the performances (by changing the position and the length of the substituents, by further β-functionalization, etc.) are attractive features of polymer **9**.

In conclusion, the regioregular insertion of nonaromatic thienyl *S*,*S*-dioxide units within the skeleton of polythiophene is a viable and versatile methodology for obtaining polymers with much greater electron affinities than those of the unmodified material. The fact that such polymers undergo reversible doping in both the n- and p-doping domains, at moderate potential values, make them attractive for a variety of applications ranging from electrochemical to electrooptical and sensing devices.

Experimental Section

Synthesis of Materials. Pd_2dba_3, $AsPh_3$, 2-(tributylstannyl)thiophene, *N*-bromosuccinimide (NBS), *N*-iodosuccinimide (NIS), and 3,4-dibromothiophene were purchased from Aldrich. 3-Chloroperoxybenzoic acid (MCPBA) (CAUTION: keep away from combustible material and avoid contact with eyes) and hydrazine (CAUTION: flammable, toxic by inhalation and in contact with skin) were purchased from Fluka. $FeCl_3$ was purchased from Carlo Erba. All solvents used in reactions and chromatographies were dried by standard procedures. 3,4-Dihexylthiophene (**2**) was prepared via nickel-catalyzed cross coupling of commercial *3*,4-dibromothiophene (**1**) with hexylmagnesium bromide[15] and the corresponding 2,5-dibromo derivative (**3**) by treating **2** with *N*-bromosuccinimide in dimethylformamide.[16]

*2,5-Dibromo-3,4-dihexylthiophene 1,1-Dioxide, **4***. To a 15-mL methylene chloride solution of 2.5 g (0.006 mol) of 2,5-dibromo-3,4-dihexylthiophene (**3**) was added stepwise 6.03 g (0.035 mol) of MCPBA (70%). The mixture was stirred overnight, filtered, and washed with a 10% $NaHCO_3$. After usual workup, the crude product was chromatographed on silica gel using hexane/ethyl acetate 95:5 (v/v) as the eluent. Yield: 1.40 g (52% yield) of a colorless crystalline product. Mp 109−110 °C. MS (70 eV, EI): *m/e* 442 ($M^{\bullet+}$); $\lambda_{max}(CHCl_3) = 352$ nm. ^1H NMR (200 MHz, $CDCl_3$, TMS): $\delta = 2.39$ (t, 4H), 1.29 (m, 16H), 0.85 (m, 6H). ^{13}C NMR (50 MHz, $CDCl_3$, TMS): $\delta = 143.3$, 115.3, 31.1, 28.9, 27.6, 27.4, 22.2, 13.8. Anal. Calcd for $C_{16}H_{26}Br_2O_2S$: C, 43.45; H, 5.93. Found C, 43.57; H, 5.94.

*3′,4′-Dihexyl-2,2′:5′,2″-terthiophene 1′,1′-Dioxide, **5***. To a 10-mL toluene solution of 0.027 g (0.026 mmol) of Pd_2dba_3 and 0.032 g (0.104 mmol) of $AsPh_3$ was added 0.77 g (1.74 mol) of **4** in 5 mL of toluene. At reflux 1.10 mL (0.0035 mol) of 2-tributylstannylthiophene was added. After refluxing for 1 h, the mixture was evaporated and the crude product chromatographed on silica gel using hexane/ethyl acetate 95:5 as the eluent. Yield: 500 mg (71% yield) of a yellow microcrystalline product. Mp: 49−50 °C. MS (70 eV, EI): *m/e* 448 ($M^{\bullet+}$); $\lambda_{max}(CHCl_3) = 412$ nm. ^1H NMR (200 MHz, $CDCl_3$, TMS): $\delta =$ 7.73 (q, $^2J(H,H) = 3.8$ Hz, $^3J(H,H) = 1.0$ Hz, 2H), 7.50 (q, $^2J(H,H) = 5.3$ Hz, $^3J(H,H) = 1.0$ Hz, 2H), 7.18 (q, $^2J(H,H) =$ 3.8 Hz, $^2J(H,H) = 5.3$ Hz, 2H), 2.65 (m, 4H), 1.40 (m, 16H), 0.90 (m, 6H). ^{13}C NMR (50 MHz, 25 °C, $CDCl_3$, TMS): $\delta =$ 137.2, 130.2, 128.7, 128.4, 127.9, 31.2, 29.5, 28.4, 26.9, 22.4, 13.9. Anal. Calcd for $C_{24}H_{32}O_2S_3$: C, 64.24; H, 7.19. Found C, 64.12; H, 7.16.

*Poly(3′,4′-dihexyl-2,2′:5′,2″-terthiophene 1′,1′-dioxide), **6***. To 0.58 g (0.0036 mol) of $FeCl_3$ in suspension in 14 mL of benzene was added 0.40 g (0.0009 mol) of **5** dissolved in 7 mL of benzene. The mixture was stirred overnight at ambient temperature and worked up with methanol, and the impurities were extracted for one night using a Soxhlet apparatus and acetone as the solvent. The violet solid residue was washed repeatedly with a 5% solution of hydrazine in water (v/v), dissolved in methylene chloride, and evaporated. Yield: 0.185 g (46% yield) of a black powder. Mp: >350 °C (upper limit of our apparatus). $\lambda_{max}(CH_2Cl_2) = 554$ nm. ^1H NMR ((200 MHz,

(15) Tamao, K.; Kodama, S.; Nakajima, I.; Kumada, M.; Minato, A.; Suzuki, K. *Tetrahedron* **1982**, *38*, 3347.

(16) Bäuerle, P.; Würthner, F.; Götz, G.; Effenberger, F.; F. *Synthesis* **1993**, 1099.

CD_2Cl_2, TMS): δ = 8.13 (d, J(H,H) = 3.7 Hz), 7.86 (d, J(H,H) = 3.7 Hz), 3.20 (m), 1.90 (m), 1.35 (m). The relative intensity ratios of the aliphatic signals were 2:8:3. The polydispersity index, measured by gel permeation chromatography using a Shodex KF-804L bar, THF as the eluent, a refractive index detector and polystyrene as the standard, was M_w/M_n = 1.4. The average molecular mass was M_n = 3799.

3″,4″-Dihexyl-2,2′:5′,2″:5″,2‴:5‴,2⁗-quinquethiophene 1″,1″-Dioxide, ***7***. To a 7-mL toluene solution of 0.0088 g (0.008 mmol) of Pd_2dba_3 and 0.001 g (0.03 mmol) of $AsPh_3$ was added 0.125 g (0.28 mmol) of 3,4-dihexyl-2,5-dibromothiophene 1,1-dioxide (**4**) in 5 mL of toluene. At reflux, 0.257 g (0.57 mmol) of 2-tributylstannyl-2,2′-bithiophene was added dropwise. The solution was stirred at reflux for 3 h and then evaporated, and the crude product was chromatographed on silica gel using hexane (91%)/ethyl acetate (6%)/methylene chloride (3%). Yield: 0.130 g of pentamer **8** (76%) as a bright red microcrystalline powder. Mp: 112 °C. MS (70 eV, EI): *m/e* 612 ($M^{\bullet+}$). λ_{max}($CHCl_3$) = 469 nm. ^{1}H NMR (200 MHz, CD_3COCD_3, TMS): δ = 7.62 (d, ^2J(H,H) = 4.0 Hz, 2H), 7.53 (q, ^2J(H,H) = 5.1 Hz, ^3J(H,H) = 1.1 Hz, 2H), 7.43 (d, ^2J(H,H) = 4.0 Hz, 4H), 7.14 (q, ^2J(H,H) = 3.7 Hz, ^2J(H,H) = 5.1 Hz, 2H), 2.80 (m, 4H), 1.60 (m, 8H), 1.40 (m, 8H), 0.90 (m, 6H). ^{13}C NMR (50 MHz, $CDCl_3$, TMS): δ = 140.1, 137.0, 136.4, 130.3, 129.8, 128.1, 127.5, 125.7, 124.7, 124.6, 31.4, 29.7, 28.6, 27.2, 22.6, 14.1 Anal. Calcd for $C_{32}H_{36}O_2S_5$: C, 62.71; H, 5.92. Found C, 62.93; H, 5.90.

2,5⁗-Diiodo-3″,4″-dihexyl-2,2′:5′,2″:5″,2‴:5‴,2⁗-quinquethiophene 1″,1″-Dioxide, ***8***. To a 50-mL solution of 0.340 g (0.56 mmol) of pentamer **7** in CH_3COOH:$CHCl_3$ 1:1 (v:v) was added stepwise 0.252 g (1.12 mmol) of *N*-iodosuccinimide at T = −20 °C, and the mixture stirred overnight at room temperature. After usual workup, the crude product was chromatographed on silica gel using a mixture of 90% hexane, 5% ethyl acetate, and 5% methylene chloride. Yield: 470 mg of **8** (98% yield) as a red powder. Mp: 148 °C. λ_{max} = 470 nm ($CHCl_3$). MS (70 eV, EI): *m/e* 864 ($M^{+\bullet}$). ^{1}H NMR (200 MHz, $CDCl_3$, TMS): δ = 7.62 (d, ^2J(H,H) =3.9 Hz, 2H), 7.19 (d, ^2J(H,H) = 3.9 Hz, 2H), 7.17 (d, ^2J(H,H) = 3.9 Hz, 2H), 6.91 (d, ^2J(H,H) = 3.9 Hz, 2H), 2.65 (t, 4H), 1.5 (m, 8H), 1.32 (m, 4H), 1.2 (m, 4H), 0.85 (m, 6H). ^{13}C NMR ($CDCl_3$, TMS): δ = 142.3, 138.7, 138.0, 137.3, 130.3, 129.8, 127.9, 125.9, 124.9, 73.2, 31.3, 29.6, 28.5, 27.2, 22.5, 14.0. Anal. Calcd for $C_{32}H_{34}I_2O_2S_5$ C, 44.45; H, 3.96. Found: C, 44.61; H, 3.97.

3‴,4‴-Dihexyl-2,2′:5′,2″:5″,2‴:5‴,2⁗:5⁗,2⁗′:5⁗′,2⁗″:5⁗″,2⁗‴-heptathiophene 1‴,1‴-Dioxide, ***10***. To a 20-mL toluene solution containing 0.00754 mmol of $Pd(AsPh_3)_4$ prepared in situ[6c] were added 0.425 g (0.5 mmol) of **8** and 0.373 g (1.0 mmol) of 2-tributylstannylthiophene. After refluxing for 4 h, the reaction mixture was evaporated, and the crude product was chromatographed using a mixture composed of 90% hexane, 5% ethyl acetate, and 5% methylene chloride. Yield: 116 mg (30% yield) of a black powder. Mp: 150 °C. λ_{max} = 505 nm (CD_2Cl_2). MS (70 eV, EI): *m/e* 776 ($M^{+\bullet}$). ^{1}H NMR (200 MHz, $CDCl_3$, TMS): δ =7.62 (d, ^2J(H,H) = 4.0 Hz, 2H), 7.31 (q, ^2J(H,H) = 5.2 Hz, ^3J(H,H) = 1.2 Hz, 2H), 7.30 (d, ^2J(H,H) = 4.0 Hz, 2H), 7.26 (q, ^2J(H,H) = 3.6 Hz, ^3J(H,H) = 1.2 Hz, 2H), 7.24 (d, ^2J(H,H) = 4.0 Hz, 2H), 7.18 (d, ^2J(H,H) = 4.0 Hz, 2H), 7.08 (q, ^2J(H,H) = 5.2 Hz, ^2J(H,H) = 3.6 Hz, 2H), 2.68 (t, 4H),1.60 (m, 12H), 1.32 (m, 4H), 0.90 (m, 6H). ^{13}C NMR (50 MHz, $CDCl_3$, TMS): δ = 139.8, 137.7, 137.0, 136.9, 135.1, 130.4, 129.9, 128.0, 127.6, 125.3, 124.9, 124.6, 124.4, 124.1, 31.2, 29.6, 28.5, 27.2, 22.5, 14.0. Anal. Calcd for $C_{40}H_{40}O_2S_7$: C, 61.82; H, 5.19. Found: C, 61.69; H, 5.21.

Poly(3″,4″-dihexyl-2,2′:5′,2″:5″,2‴:5‴,2⁗:5⁗,2⁗′-quinquethiophene 1″,1″-dioxide), ***9***. To 0.42 g (0.0026 mol) of $FeCl_3$ in suspension in 10 mL benzene was added dropwise 0.41 g (0.000 66 mol) of **7** dissolved in 7 mL of benzene. The mixture was stirred overnight at ambient temperature, worked up with methanol, dried, and then extracted using a Soxhlet apparatus, 1 day with methanol and 1 day with acetone as the solvents. The solid residue was washed repeatedly with a 5% solution of hydrazine in water (v/v). Yield: 390 mg of a black powder, scarcely soluble in organic solvents. Mp: >250 °C (upper limit of our apparatus). Repeated washing of the powder with hot methylene chloride afforded 5 mg of a black powder (mp 210 °C) characterized by the following proton spectrum: ^{1}H NMR (400 MHz, CD_2Cl_2, TMS): δ = 7.62 (q, ^2J(H,H) = 3.0 Hz, ^3J(H,H) = 2.0 Hz, 2H), 7.31 (q, ^3J(H,H) = 4.2 Hz, ^3J(H,H) = 3.0 Hz, 2H), 7.11 (q, ^3J(H,H) = 4.2 Hz, 2.0 Hz, 2H), 7.14 (d, ^2J(H,H) = 4.5 Hz, 2H), 6.84 (d, ^2J(H,H) = 4.5 Hz, 2H), 7.32 (s, 8H), 7.22 (d, ^2J(H,H) = 2.0 Hz, 2H), 7.26 (d, ^2J(H,H) = 2.0 Hz, 2H), 2.68 (t, 8H), 1.60 (m, 24H), 1.32 (m, 8H), 0.90 (m, 12H). By comparison with the spectrum of heptamer **10**, the spectrum was assigned to the decamer "dimer" of compound **7**.

Electrochemical Measurements. The electrochemical syntheses of polymers **6**, **9**, and **11** were performed under several different conditions on Pt (0.13 cm^2) and on tin oxide-coated glass (∼1 cm^2). The electrochemical and spectroelectrochemical measurements were performed with an EG&G PAR M270A potentiostat/galvanostat and a Perkin-Elmer Lambda 19 spectrometer. All chemicals were reagent-grade products purified before use. Electrochemical experiments were performed in a Labmaster 130 Mbraun drybox (oxygen and water contents < 1 ppm) at room temperature. Quasi reference electrodes Ag/AgCl were used and all the potential data were then calculated vs SCE.

Theoretical Calculations. All calculations were carried out utilizing HyperChem implementation.[17] Frontier orbitals and UV transitions were calculated by 4 × 4 singly excited CI single ZINDO/S calculations on PM3 optimized geometries.

Acknowledgment. The present work was supported by MURST (Electrochemical and Electronic Devices with Polymer Components) and University of Bologna (funds for selected research topics).

CM990245E

(17) *HyperChem* rel. 4.5 from Hypercube, Inc. Waterloo, Ontario, Canada.